Size-Dependent Grain-Growth Kinetics Observed in Nanocrystalline Fe

C. E. Krill III,[1,*] L. Helfen,[1] D. Michels,[1] H. Natter,[2] A. Fitch,[3] O. Masson,[3] and R. Birringer[1]

[1]*FR 7.3 Technische Physik, Gebäude 43, Universität des Saarlandes, Postfach 151150, D-66041 Saarbrücken, Germany*

[2]*FR 8.13 Physikalische Chemie, Gebäude 9, Universität des Saarlandes, Postfach 151150, D-66041 Saarbrücken, Germany*

[3]*ESRF, BP 220, F-38043 Grenoble Cedex, France*

(Received 22 September 2000)

Measurements of grain growth in nanocrystalline Fe reveal a linear dependence of the grain size on annealing time, contradicting studies in coarser-grained materials, which find a parabolic (or power-law) dependence. When the grain size exceeds ~150 nm, a smooth transition from linear to nonlinear growth kinetics occurs, suggesting that the rate-controlling mechanism for grain growth depends on the grain size. The linear-stage growth rate agrees quantitatively with a model in which boundary migration is controlled by the redistribution of excess volume localized in the boundary cores.

DOI: 10.1103/PhysRevLett.86.842 PACS numbers: 81.40.Ef, 65.80.+n, 81.07.Bc, 81.10.–h

Since the network of grain boundaries in a polycrystalline material is a source of excess energy relative to the single-crystalline state, there is a thermodynamic driving force for reduction of the total grain-boundary area or, equivalently, for an increase in the average crystallite (grain) size $\bar{R}$ [1]. According to classical models for the technologically important process of grain growth, the rate at which $\bar{R}$ increases is governed by the intrinsic grain-boundary mobility, which depends strongly on temperature, and by such factors as defect concentrations, second-phase precipitates, and the segregation of impurity atoms to the boundary cores [1,2]. Since all of these parameters are independent of $\bar{R}$, the classical models assume that a single growth mechanism is rate controlling at all length scales.

Measurements of grain-growth kinetics in conventional polycrystalline samples ($\bar{R} \gtrsim 1\ \mu$m) have uncovered no exceptions to the latter assumption; however, studies performed in nanocrystalline materials ($\bar{R} \lesssim 100$ nm) have found the growth rate to be much slower than that entailed by an extrapolation from the coarse-grained regime [3,4]. The prevailing view has attributed this unexpected slowdown to the solute drag resulting from impurities introduced during the preparation of nanocrystalline samples.

It, therefore, comes as a surprise that recent theoretical considerations present a compelling case for an enhanced intrinsic stability with respect to coarsening in materials with nanometer-sized grains, even in the absence of significant impurity concentrations [5–9]. These theoretical models posit the existence of a critical grain size $\bar{R}_c$—generally thought to lie in the submicron range—below which the rate-controlling step for grain-boundary migration is not the boundary-curvature-driven diffusion of atoms across and along the boundary cores (as in conventional, coarse-grained materials [2]) but rather the migration and/or rearrangement of other features associated with the grain boundaries, like the triple junctions (intersections of three or more grain boundaries) [5,6] or the excess volume localized in the core regions [7–9]. A feature common to such models is the prediction of a linear dependence of $\bar{R}$ on annealing time t when $\bar{R} < \bar{R}_c$ and a crossover at $\bar{R} = \bar{R}_c$ to the nonlinear growth kinetics familiar from studies of grain growth in conventional materials [1,2]. The models differ, however, with respect to the predicted temperature dependence of the small-$\bar{R}$ growth kinetics, because the latter depends sensitively on details of the rate-controlling step for boundary migration. By exploiting this difference, one may be able to distinguish experimentally between competing models for grain growth in nanocrystalline materials.

The goal of the experiments described in this Letter was to test the predictions of these new models by performing detailed measurements of grain-growth kinetics in a highly pure, elemental nanocrystalline sample. To this end, nanocrystalline Fe was prepared using the technique of mechanical attrition [4,10]. The initial powder (99.99+% metallic purity) was purified by annealing under hydrogen gas and then milled for 24 h under Ar in a SPEX 8000 mixer/mill outfitted with a steel vial and balls, a procedure that produced fully dense powder particles exceeding 50 μm in diameter, each containing crystallites (grains) with an average (area-weighted) size $\bar{R}$ of 35 nm. The total impurity concentration of the milled powder was less than 0.3 at. % (primarily oxygen). Although it is possible to study the isothermal time evolution of $\bar{R}$ in such a sample by means of the same method used to measure grain growth in conventional materials—sequential steps of annealing followed by microstructural characterization via optical or electron microscopy—this would not provide the high time resolution necessary to establishing the functional form of $\bar{R}(t)$ during the initial stage of grain growth or the occurrence of a change in functional form at $\bar{R}_c$. We have found that such information can be obtained by means of a novel x-ray diffraction method that exploits the high angular resolution and high intensity of the powder-diffractometer beam line BM16 at

 0031-9007/01/86(5)/842(4)$15.00

the European Synchrotron Radiation Facility (ESRF) [11]. Samples of ball-milled Fe powder sealed in quartz capillaries were heated *in situ* by a hot-air blower while a multichannel detector was scanned continuously over an angular range encompassing the first four Bragg peaks. The average grain size in the sample could be determined by means of a Fourier analysis [12–14] of the (110) and (220) peak profiles at time intervals as short as 2 min. In this manner it was possible to gain near-real-time grain-size information during the initial stage of grain growth in the nanocrystalline powder at several different annealing temperatures.

The isothermal evolution of the grain size in ball-milled Fe is plotted for several annealing temperatures in Fig. 1. Within the first 2 min of annealing, $\bar{R}$ increases rapidly to nearly twice the as-milled grain size; owing to the thermal equilibration time of about 5 min, this initial growth spurt could not be characterized more precisely. We ignore it in the subsequent analysis for reasons discussed below. Following the initial jump in $\bar{R}$, the growth rate slows substantially and appears to take on an approximately linear time dependence at all grain sizes below about 150 nm. Above this grain size, the growth rate slows further, and the $\bar{R}(t)$ curves manifest the nonlinear power-law behavior characteristic of curvature-driven grain growth in conventional materials [1,2].

We will see shortly that these results are in quantitative agreement with the predictions of a model developed by Estrin and colleagues [7–9] contending that, at sufficiently small grain sizes, the rate-controlling step for boundary migration becomes the transport of excess volume away from the moving boundaries. We now summarize the main features of this model before examining its consistency with the measurements of Fig. 1. Because the core of a grain boundary is less dense than its adjacent crystalline regions,

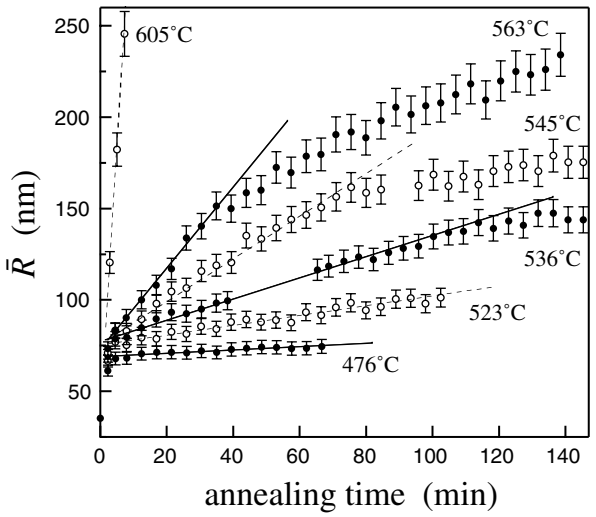

FIG. 1. Isothermal evolution of $\bar{R}$ in ball-milled, nanocrystalline Fe at the indicated annealing temperatures, as determined by a Fourier analysis of x-ray diffraction peak profiles. The straight lines are guides to the eye illustrating linear growth kinetics at initial annealing times; deviations from linearity become apparent when $\bar{R}$ exceeds ~150 nm.

grain boundaries are locations of excess volume δV relative to the single-crystalline state. Since grain growth entails a reduction in the total grain-boundary area A, the excess volume localized in the annihilated boundary area must be accommodated elsewhere in the sample or transported to the surface. According to recent computer simulations performed by Upmanyu *et al.* [15], much of the excess volume freed during grain growth is initially incorporated into nearby crystalline regions in the form of vacancies, leading to a nonequilibrium vacancy concentration and a concomitant increase in the free energy G, which counteracts the decrease in G associated with the reduction in A [7,8]. Estrin *et al.* [7–9] showed that, as long as $\bar{R}$ is smaller than a critical size $\bar{R}_c$, this vacancy-generation-induced reduction in the overall driving force for grain growth leads to a dramatic slowdown in growth kinetics and an approximately linear increase in $\bar{R}$ (equivalent-sphere diameter) with annealing time according to

$$\bar{R}(t) = \bar{R}_0 + \frac{\gamma D_{\mathrm{SD}}}{12 N k_B T Z[(\delta V)/A]^2}\, t \qquad (\bar{R} < \bar{R}_c), \quad (1)$$

with initial grain size $\bar{R}_0$, temperature T, Boltzmann constant k_B, and the following material parameters: grain-boundary energy γ, bulk self-diffusion coefficient D_{SD}, number of atoms per unit volume N, and atomic coordination number Z. When $\bar{R}$ is greater than $\bar{R}_c$, the production of excess vacancies is no longer rate determining for boundary motion, and the classical parabolic growth kinetics obtain:

$$\bar{R}^2(t) = \bar{R}_0^2 + 8 m \gamma t \qquad (\bar{R} \gtrsim \bar{R}_c), \quad (2)$$

where m denotes the grain-boundary mobility [1,2]. The critical grain size $\bar{R}_c$ separating the ranges of validity of Eqs. (1) and (2) is determined by equating their respective time derivatives:

$$\bar{R}_c = 48 N k_B T Z[(\delta V)/A]^2 m / D_{\mathrm{SD}}. \quad (3)$$

Inserting typical values for aluminum into the right-hand side of Eq. (3), Estrin *et al.* [9] estimated $\bar{R}_c \approx 200$ nm, suggesting that the initial grain growth in nanocrystalline materials is governed by Eq. (1) rather than Eq. (2).

Although the linear growth evident in Fig. 1 is consistent with the predictions of the model, the linearity could be an artifact of the small range in grain sizes over which the initial growth stage seems to extend—that is, the grain-size evolution at $\bar{R} < 150$ nm may actually follow Eq. (2) with an imperceptibly small curvature. A clear distinction between linear and nonlinear growth kinetics can nevertheless be drawn by examining the temperature dependence of the measured growth rates. In Eq. (2) temperature enters the rate of growth primarily through the boundary mobility m, which can be written as

$$m(T) = \frac{m_0}{T} \exp(-Q_{\mathrm{mig}}/k_B T), \quad (4)$$

where m_0 is a constant and Q_{mig} is an effective activation energy for boundary migration [16]; in experimental studies of grain growth in coarse-grained polycrystalline

materials, Q_{mig} is usually found to take on values close to the activation energy for grain-boundary diffusion [2]. According to Eq. (1), the rate of grain growth in the linear region is proportional to D_{SD}, the temperature dependence of which can be expressed in Arrhenius form:

$$D_{\mathrm{SD}}(T) = D_0 \exp(-Q_{\mathrm{SD}}/k_B T), \tag{5}$$

where D_0 is a constant and Q_{SD} is the activation energy for self-diffusion in the given material [17]. Since the latter quantity is typically at least twice as large as the activation energy for grain-boundary diffusion [2], we expect $Q_{\mathrm{SD}} \gg Q_{\mathrm{mig}}$; thus, when grain growth is controlled by the redistribution of excess volume, the activation energy should be much higher than that of grain growth in a coarse-grained specimen of the same material.

Substituting Eqs. (4) and (5) into Eqs. (2) and (1), respectively, we find that in both cases the initial growth rate $(d\bar{R}/dt)_{t\to 0}$ is proportional to $T^{-1}\exp(-Q/k_B T)$, with Q representing Q_{SD} or Q_{mig}. Thus, a value for the activation energy governing the initial stage of coarsening can be determined from the slope of an Arrhenius plot of the initial growth rate multiplied by the annealing temperature. Figure 2 represents such a plot for the growth curves of Fig. 1. All data points in Fig. 2 lie along a straight line, except at the lowest annealing temperatures near 475 °C. A weighted least-squares fit of a straight line (dashed line in Fig. 2) yields an apparent activation energy $Q = 330 \pm 15$ kJ/mol. Considering that the expected value for Q_{mig}, namely, the activation energy for grain-boundary diffusion in Fe, is 174 kJ/mol [18], we can rule out grain-boundary diffusion of Fe as the rate-controlling step for the initial

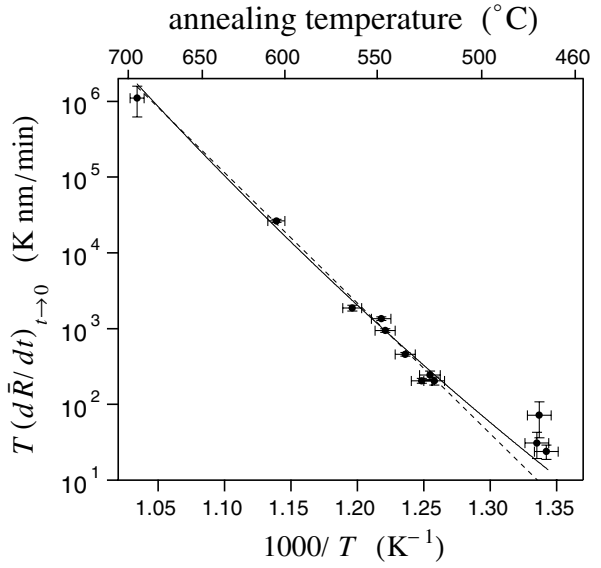

FIG. 2. Arrhenius plot of the initial growth rate in nanocrystalline Fe for the data of Fig. 1 and additional annealing temperatures. The dashed line is a weighted least-squares fit of a straight line to the data, which yields an apparent activation energy of 330 kJ/mol; the solid curve is a fit of Eq. (1) with adjustable parameter $(\delta V)/A$. The optimal value for the latter quantity is found to be 0.019 nm.

coarsening of ball-milled Fe. At first glance, the data of Fig. 2 appear to be inconsistent with the excess-volume model, as well, since Q_{SD} for Fe is typically quoted as 251–282 kJ/mol [18]. However, the latter value is valid only at temperatures above the Curie transition in Fe; below $T_C = 770$ °C magnetic ordering imparts an additional temperature dependence to the exponential term in Eq. (5), causing Q_{SD} to exceed its value in paramagnetic Fe [19].

In order to test the consistency of the excess-volume model with the data of Fig. 2, we must, therefore, insert the full temperature dependence of D_{SD} for Fe [20] into Eq. (1) along with the known values for N, γ [21], and Z. The solid line in Fig. 2 is a least-squares fit of the resulting expression for $T(d\bar{R}/dt)_{t\to 0}$, which contains a single adjustable parameter: the average excess volume per unit area, $(\delta V)/A$, in the boundary core region. The fit yields a value of 0.019 ± 0.001 nm for $(\delta V)/A$, which compares favorably with experimental values ranging from 0.01 to 0.04 nm for special boundaries in bicrystals [22], and a value of $\sim$0.02 nm for high-angle boundaries in nanocrystalline Pd [23]. The curvature of the fit function arises entirely from the temperature dependence of D_{SD}, and it closely mirrors the curvature evident in the data. Note that the excess-volume model accounts not only for this curvature but also for the absolute magnitude of the data points, since the range of physically reasonable values for $(\delta V)/A$ severely restricts the position of the fit curve in Fig. 2 with respect to the vertical axis. Thus, the initial coarsening rates in ball-milled Fe are predicted remarkably well by the excess-volume model, suggesting that the enhanced thermal stability in this material can be explained without appealing to solute drag.

As noted above, an alternative model based on the mobility of triple junctions can also account for the occurrence of linear grain growth at small grain sizes [5,6]. In this case the measured activation energy would correspond to that of triple-junction migration, Q_{TJ}. If the average value for Q_{TJ} in Fe happens to be equal to Q_{SD}, then the data of Fig. 2 cannot rule out the possibility that triple-junction migration is the rate-controlling step for grain growth in ball-milled Fe. However, even though there is no known general relation between Q_{TJ} and Q_{SD} for polycrystalline materials, it seems improbable that these two quantities would be equal over the entire temperature range studied in these experiments.

Finally, we return to the rapid growth observed in the first few minutes of each of the annealing treatments. Analysis of the x-ray diffraction peak profiles reveals that the microstrain present in the nanocrystalline grains decreases from a high level of 0.4% in the as-milled state to under 0.1% in only $\sim$2 min. Microstrain in ball-milled Fe is known to be caused primarily by dislocations [24], suggesting that the dislocation density decreases rapidly once the grains begin to grow. Since the onset of linear growth kinetics coincides with the drop in microstrain to negligibly small levels, we believe that the presence of dislocations in the as-milled powder is responsible for the initially

rapid growth. This is consistent with the excess-volume model, because the value of the critical size $\bar{R}_c$ depends on the spacing of sinks for the excess vacancies generated during boundary annihilation [7]; in the derivation of Eq. (1) it was assumed that only the grain boundaries act as vacancy sinks. If the cores of the dislocations in the as-milled grains act as additional vacancy sinks, then $\bar{R}_c$ takes on a value well below $\bar{R}$, with the result that the initial growth rate is governed by Eq. (2) rather than Eq. (1). During the initial burst of grain growth, the dislocation density drops precipitously, causing $\bar{R}_c$ to increase above $\bar{R}$ and linear growth kinetics to obtain until the grain size exceeds the dislocation-free value for $\bar{R}_c$.

Thus, the kinetics of coarsening in ball-milled Fe are consistent with the main features of the excess-volume model developed by Estrin *et al.* [7–9]: linear growth kinetics at small grain sizes, an activation energy for boundary migration equal to that of self diffusion, a transition to nonlinear kinetics at a grain size on the order of 150 nm, and a physically plausible value for the excess volume per unit grain-boundary area, $(\delta V)/A = 0.019 \pm 0.001$ nm. Furthermore, the initial growth rate measured in nanocrystalline Fe agrees quantitatively with the model, suggesting that, in addition to the appearance of grain-size-dependent growth kinetics, the redistribution of excess volume localized in the boundary cores can account for the anomalously high stability with respect to coarsening observed in nanocrystalline samples.

We are grateful to G. Gottstein for suggesting that excess-volume redistribution may be relevant to our measurements of growth kinetics in nanocrystalline materials and to Y. Estrin, D. Molodov, E. Rabkin, and L. S. Shvindlerman for helpful comments and discussion. We thank M. Schmelzer for experimental assistance and the Deutsche Forschungsgemeinschaft [SFB 277 and Habilitation fellowship (CEK)] and ESRF for financial support.

*Corresponding author.
Email address: krill@rz.uni-sb.de

[1] H. V. Atkinson, Acta Metall. **36**, 469 (1988).
[2] F. J. Humphreys and M. Hatherly, *Recrystallization and Related Annealing Phenomena* (Pergamon Press, Oxford, 1996), Chaps. 4 and 9.
[3] R. W. Cahn, in *Physical Metallurgy,* edited by R. W. Cahn and P. Haasen (North-Holland, Amsterdam, 1996), 4th ed., Vol. 3, Chap. 28, pp. 2399–2500.
[4] T. R. Malow and C. C. Koch, Acta Mater. **45**, 2177 (1997).
[5] U. Czubayko, V. G. Sursaeva, G. Gottstein, and L. S. Shvindlerman, Acta Mater. **46**, 5863 (1998).
[6] U. Czubayko, V. G. Sursaeva, G. Gottstein, and L. S. Shvindlerman, in *Grain Growth in Polycrystalline Materials III,* edited by H. Weiland, B. L. Adams, and A. D. Rollett (The Minerals, Metals & Materials Society, Warrendale, PA, 1998), pp. 423–430.
[7] Y. Estrin, G. Gottstein, and L. S. Shvindlerman, Scr. Mater. **41**, 385 (1999).
[8] Y. Estrin, G. Gottstein, and L. S. Shvindlerman, Acta Mater. **47**, 3541 (1999).
[9] Y. Estrin, G. Gottstein, E. Rabkin, and L. S. Shvindlerman, Scr. Mater. **43**, 141 (2000).
[10] A. Michels, C. E. Krill, H. Natter, and R. Birringer, in *Grain Growth in Polycrystalline Materials III* (Ref. [6]), pp. 449–454.
[11] A. N. Fitch, Mater. Sci. Forum **228–231**, 219 (1996).
[12] B. E. Warren, *X-Ray Diffraction* (Addison-Wesley, Reading, MA, 1969), Chap. 13.
[13] C. E. Krill and R. Birringer, Philos. Mag. A **77**, 621 (1998).
[14] C. E. Krill, R. Haberkorn, and R. Birringer, in *Spectroscopy and Theory,* Handbook of Nanostructured Materials and Nanotechnology Vol. 2, edited by H. S. Nalwa (Academic Press, San Diego, 2000), Chap. 3, pp. 155–211.
[15] M. Upmanyu, D. J. Srolovitz, L. S. Shvindlerman, and G. Gottstein, Interface Sci. **6**, 287 (1998).
[16] L. C. Chen and F. Spaepen, J. Appl. Phys. **69**, 679 (1991).
[17] J. L. Bocquet, G. Brebec, and Y. Limoge, in *Physical Metallurgy,* edited by R. W. Cahn and P. Haasen (North-Holland, Amsterdam, 1996), 4th ed., Vol. 1, Chap. 7, pp. 535–668.
[18] *Smithells Metals Reference Book,* edited by E. A. Brandes and G. B. Brook (Butterworth-Heinemann, London, 1992), 7th ed., Chap. 13, pp. 12, 117.
[19] G. Hettich, H. Mehrer, and K. Maier, Scr. Metall. **11**, 795 (1977).
[20] M. Lübbehusen and H. Mehrer, Acta Metall. Mater. **38**, 283 (1990).
[21] J. W. Taylor, J. Inst. Met. **86**, 456 (1957/1958).
[22] A. P. Sutton and R. W. Balluffi, *Interfaces in Crystalline Materials* (Clarendon Press, Oxford, 1995), p. 353.
[23] R. Birringer, C. E. Krill, and M. Klingel, Philos. Mag. Lett. **72**, 71 (1995).
[24] Á. Révész, T. Ungár, A. Borbély, and J. Lendvai, Nanostruct. Mater. **7**, 779 (1996).